Supporting information

Efficient and stable electrocatalyst for methanol oxidation reaction based on Pt-Au-Ag tri-metallic nanodendrite

Experimental Section

All chemicals including $HAuCl_4$, (99.999%), K_2PtCl_4 (99.9%), $AgNO_3$ (99.9%), and citric acid were purchased from Sigma-Aldrich. Electrochemical synthesis of Ag nanodendrites was performed on a galvanostat (Epsilon, Bioanalytical Chemistry Systems, Inc, USA). Initially, a Ti substrate (1 cm^2) was immersed in a solution composed of 10 mM $AgNO_3$ and 1 M citric acid. Then, a current of 600 μA was applied for electrodeposition of Ag over 15 minutes. To construct Pt-Au-Ag trimetallic nanodendrites, Ag nanodendrites were immersed in a solution containing $AuCl_4^-$ and $PtCl_4^{2-}$, and both GRRs were simultaneously executed at 100°C with stirring. The atomic composition of the trimetallic nanodendrites was varied by changing the GRR reaction times as well as the $AuCl_4^-$ and $PtCl_4^{2-}$ concentrations.

SEM images and energy-dispersive X-ray (EDX) spectra of the synthesized nanodendrite structures were acquired using a Hitachi S-4800 scanning electron microscope. TEM and high-resolution TEM (HRTEM) images were obtained using a JEM-2100F transmission electron microscope (JEOL, Japan) with an accelerating voltage of 200 KV. X-ray diffraction (XRD) was measured using a D/MAX Rint 2000 diffractometer (Rigaku, Japan) with CuKα radiation (λ = 1.54178 Å, 40 KV and 200 mA). Elemental mapping was performed by EDS (Oxford, UK) using a 1.5 nm probe and images were constructed using INCA software.

All electrochemical measurements in this study were performed at room temperature using a standard cell with three electrode arrangements in which Ag/AgCl (3M KCl) and Pt wire were used as reference and counter electrodes, respectively. The potential measurement was performed relative to the reference electrode and all electrochemical data were recorded using a potentiostat (BAS 100B, Bioanalytical Systems, Inc., USA).

To calculate EASA, CVs for the tested structures were acquired in a 0.5 M H_2SO_4 solution at a scan rate of 50 mV/s (Figure S6). Two reduction peaks at -0.15 and -0.05V were used to calculate Q_H, and Q_S was assumed to 230 μC/cm^2 based on previous researches. [1-3] MOR was executed in a solution composed of 0.5 M CH_3OH and 0.2 M H_2SO_4. Dissolved O_2 and CO_2 in the solution were completed removed by thorough N_2 bubbling. Cyclic voltammetry (CV) was performed during MOR, and the resulting electrochemical signals were measured. For the comparison with the tested electrodes, a bare Pt electrode (99.99%) with a geometric area of 1×1 cm^2 was also prepared.

Tunable composition of Pt-Au-Ag trimetallic nanodendrite

Galvanic replacement reactions (GRRs) for synthesis of Pt-Au-Ag trimetallic nanodendrite:

$4Ag + AuCl_4^- \rightleftharpoons Au + 4AgCl$ (1)

$4Ag + PtCl_4^{2-} \rightleftharpoons Pt + 4AgCl$ (2)

Both GRRs (1) and (2) were performed in a solution (100^{o}C) composed of 0.2 mM HCl, 0.5 M polyvinyl pyrrolidone (PVP), 5 mM $AuCl_4^-$, and 5 mM $PtCl_4^{2-}$ with continuous stirring (Corresponding to the trimetallic structure in Figure 2). PVP was used as a catalyst to drive the formation of a multi-metallic nanostructure with a uniform and homogeneous composition, as demonstrated in a previous study.[1] HCl was used to precipitate AgCl faster. Precipitate on the surface was carefully removed in a saturated NaCl solution and then rinsed in de-ionized water with stirring.

To demonstrate compositional tunability, we fabricated a trimetallic nanodendrite by increasing the concentration of $AuCl_4^-$ from 5 to 8 mM, while keeping the other conditions unchanged. A TEM image (a) of the synthesized trimetallic nanodendrite and the corresponding elemental mappings of Pt (b), Au (c), and Ag (d) are shown in Figure S1. Elemental mapping results again verified that each metal was homogeneously distributed throughout the nanodendrite. The denser green color indicates a higher concentration of Au in this nanodendrite than the one synthesized using 5 mM $AuCl_4^-$. We superimposed line mappings across the structure on the TEM image. Again, the peak intensities of the three metals changed similarly along the line and the intensity of Au (green) was the strongest. The atomic concentrations of Pt, Au, and Ag were 20.0, 46.0, and 34.0%, respectively, based on the EDAX analysis, confirming an elevated Au concentration in comparison with that of the nanodendrite shown in Figure 2.

Another tri-metallic nanodendrite structure was prepared by decreasing the $AuCl_4^-$ concentration to 3 mM and increasing the $PtCl_4^{2-}$ concentration to 15 mM. Simultaneously, the reaction time was increased from 8 to 15 minutes. Figure S2 shows a TEM image (a) of the synthesized nanodendrite structure and the corresponding elemental mappings of Pt (b), Au (c), and Ag (d). An increase in the concentration of Pt and decrease in the concentration of Au was clearly evident, and the determined atomic concentrations of Pt, Au, and Ag were 57.0, 14.0, and 29.0%, respectively. Peaks of Pt, Au, and Ag along the mapping line were overlaid on the TEM image. The intensity of Pt was higher than those of Au and Ag due to the use of a high concentration of $PtCl_4^{2-}$ in the GRR.

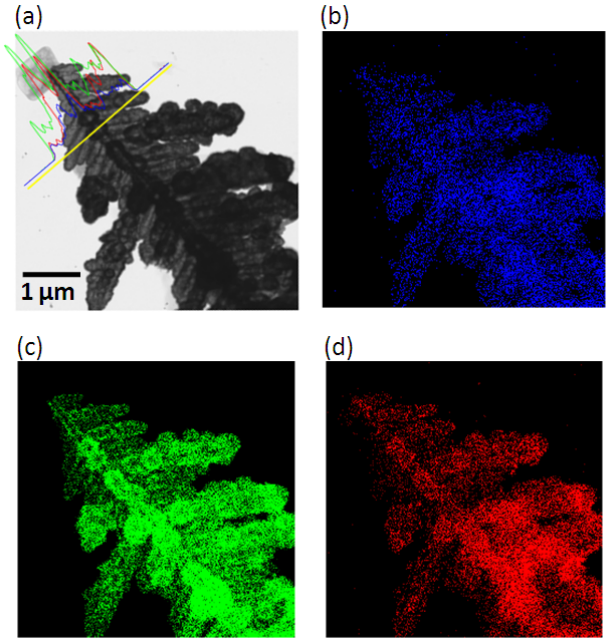

Figure S1. TEM image of a single Pt-Au-Agnanodendrite (a) composed of 20.0% Pt, 46.0% Au, and 34.0% Ag. Line mappings that cross the pivot of the nanodendrite is overlaid on the image. Blue, green, and red indicate the intensity variation of Pt, Au and Ag, respectively. Elemental mappings of Pt (blue, (b)), Au (green, (c)) andAg (red, (d)) performed separately for the nanodendrite are also shown.

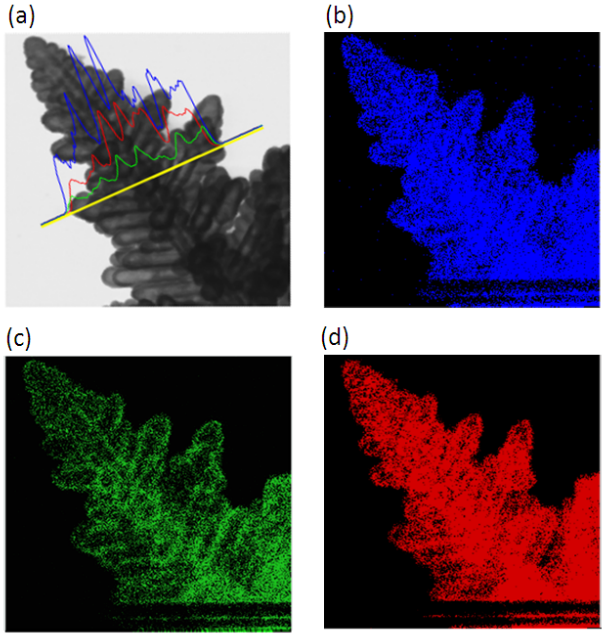

Figure S2. TEM image of a single Pt-Au-Ag nanodendrite (a) composed of 57.0% Pt, 14.0% Au, and 29.0% Ag. Line mappings crossing the pivot of the nanodendrite are overlaid. Blue, green, and red indicate the intensity variation of Pt, Au, and Ag, respectively. Elemental mappings of Pt (blue, (b)), Au (green, (c)), and Ag (red, (d)) performed separately for the nanodendrite are also shown.

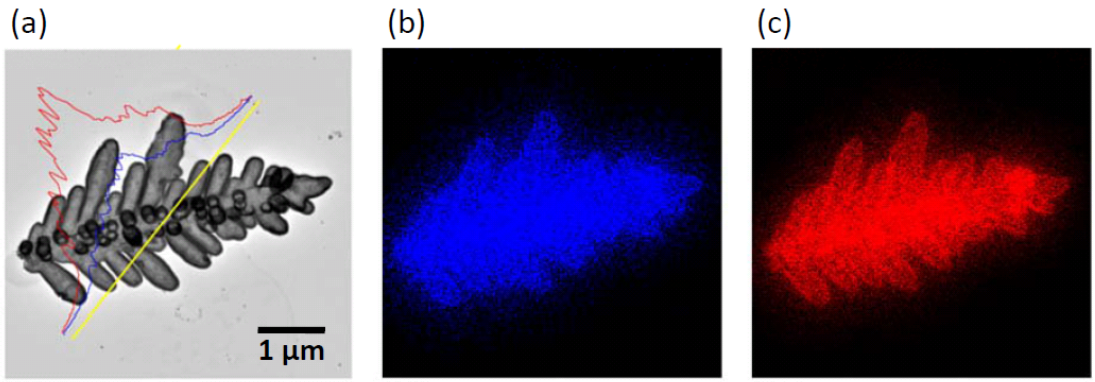

Figure S3. TEM image of a Pt-Ag nanodendrite (a) and overlaid line mappings crossing the nanodendrite. Blue and red colors indicate the intensity variation of Pt and Ag, respectively. Elemental mappings of Pt (blue, (b)) and Ag (red, (d)) on the nanodendrite are also shown.

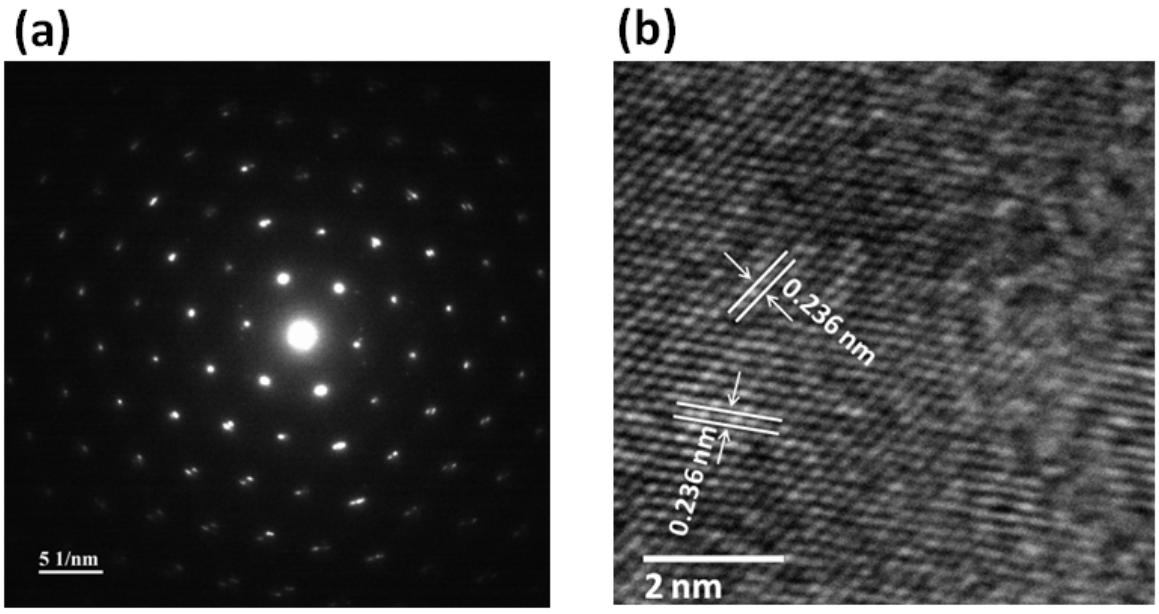

Figure S4. Selected area electron diffraction (SAED, (a)) and high-resolution TEM (HRTEM) images (b) of the trimetallic nanodendrite presented in Fig. 2 (a). The HRTEM image indicates that the nanodendrite has a lattice structure with an inter-distance of 0.236 nm.

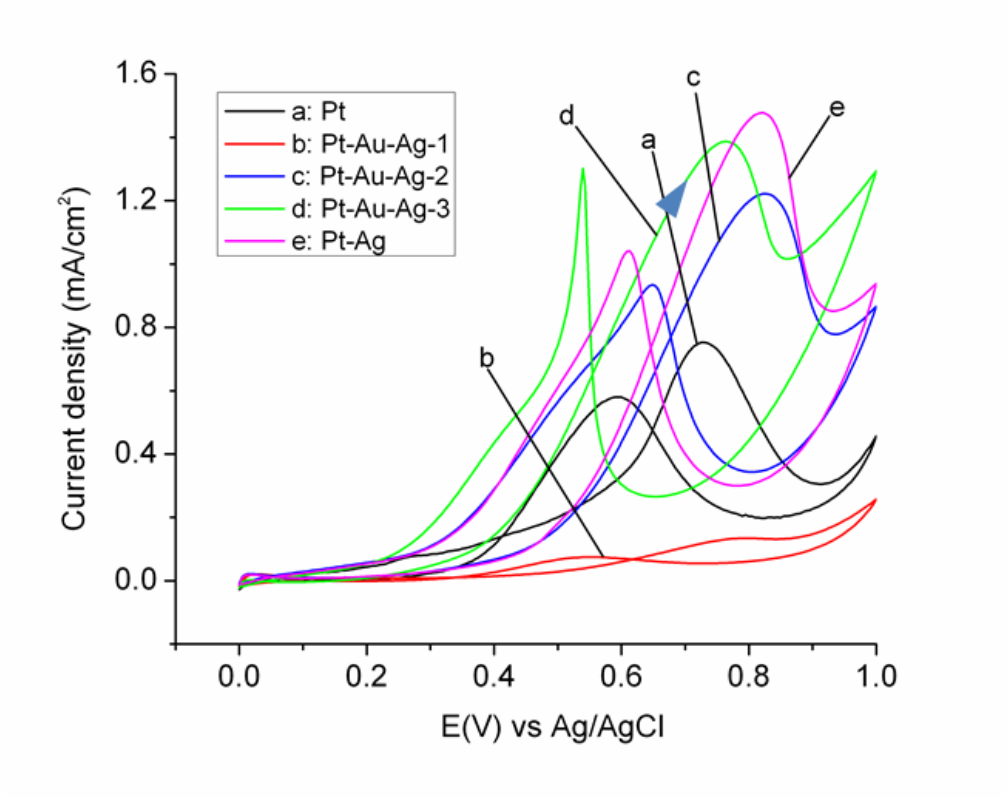

Figure S5. CVs of MOR acquired in an aqueous solution containing 0.5 M methanol and 0.2 M H_2SO_4, using five different structures (scan rate: 50 mV/s)

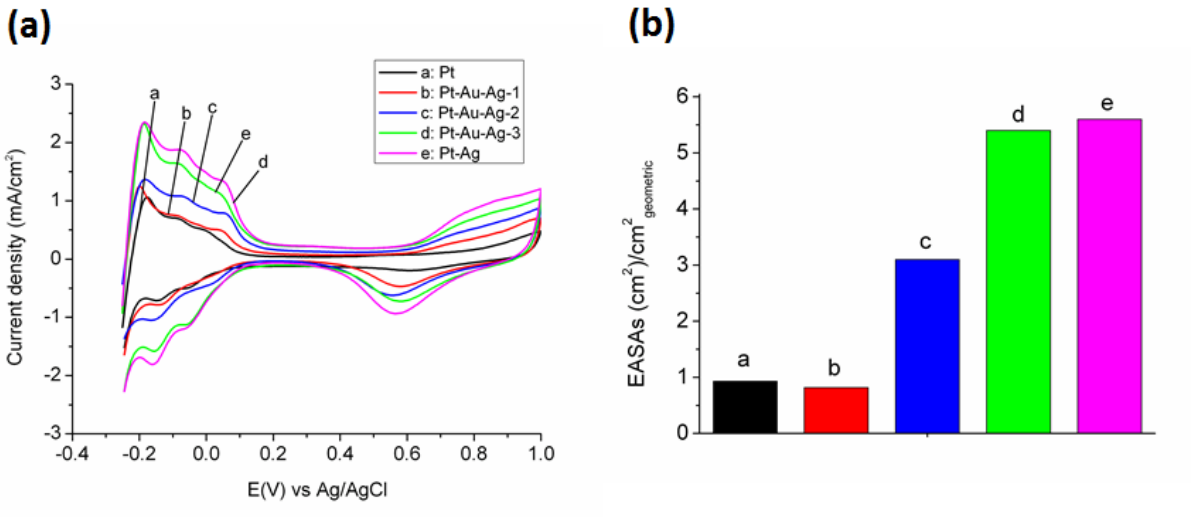

Figure S6. (a) CVs acquired in a 0.5 M H_2SO_4 solution at a scan rate of 50 mV/s using the same five structures presented in Fig. 4 and (b) EASAs for the corresponding electrodes.

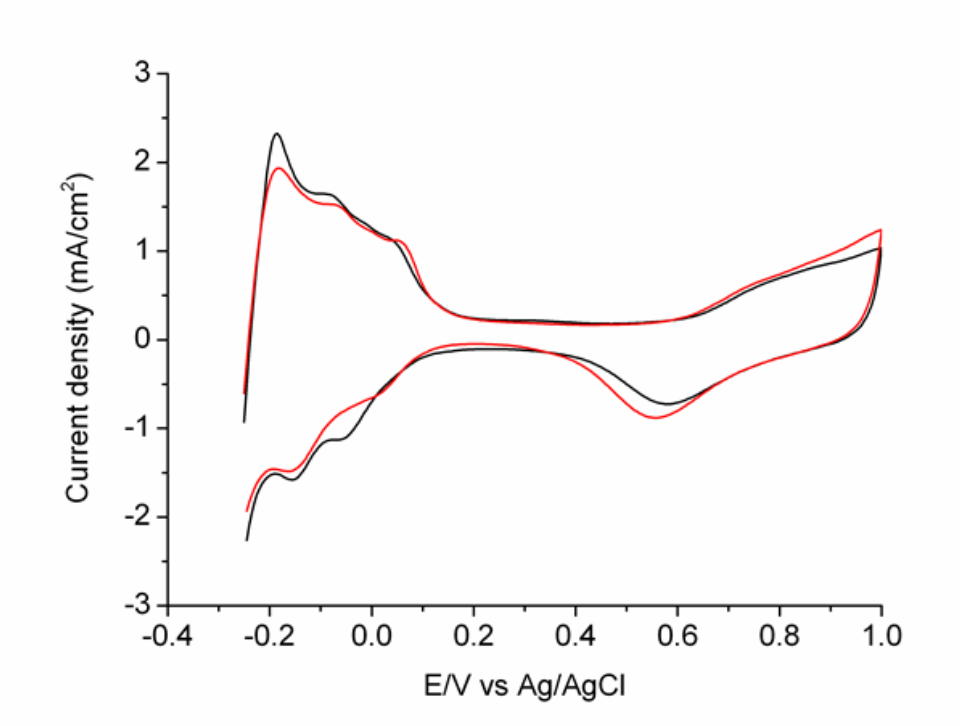

Figure S7. CVs acquired in a 0.5 M H_2SO_4 solution at a scan rate of 50 mV/s using Pt-Au-Ag-3 electrode before (black) and after (red) 20 minutes MOR reaction (conditions similar to those used for figure 4b).

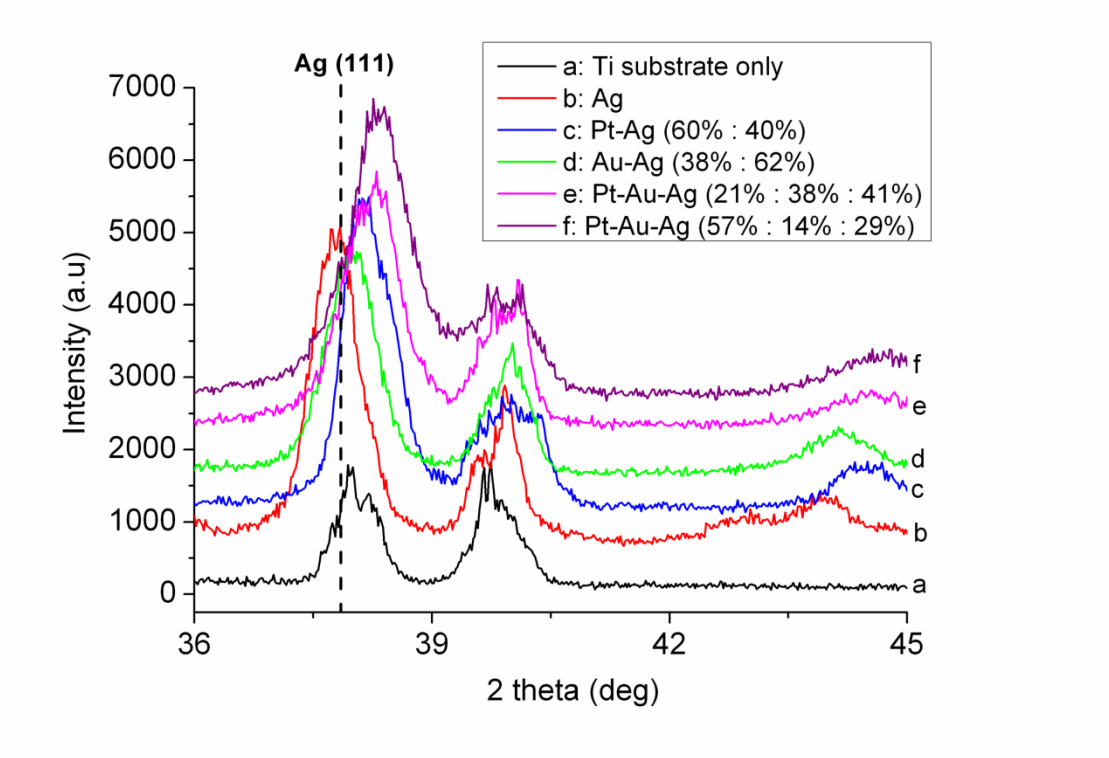

Figure S8. Magnification of XRD patterns from Fig. 3